



HAL
open science

Tailoring the Schiff Base Photoswitching -non- adiabatic molecular dynamics study of substituent effect on Excited State Proton Transfer †

Joanna Jankowska, Mario Barbatti, Joanna Sadlej, Andrzej Sobolewski

► To cite this version:

Joanna Jankowska, Mario Barbatti, Joanna Sadlej, Andrzej Sobolewski. Tailoring the Schiff Base Photoswitching -non- adiabatic molecular dynamics study of substituent effect on Excited State Proton Transfer †. *Physical Chemistry Chemical Physics*, 2017, 19 (7), pp.5318-5325. 10.1039/c6cp08545h . hal-02288759

HAL Id: hal-02288759

<https://amu.hal.science/hal-02288759>

Submitted on 16 Sep 2019

HAL is a multi-disciplinary open access archive for the deposit and dissemination of scientific research documents, whether they are published or not. The documents may come from teaching and research institutions in France or abroad, or from public or private research centers.

L'archive ouverte pluridisciplinaire **HAL**, est destinée au dépôt et à la diffusion de documents scientifiques de niveau recherche, publiés ou non, émanant des établissements d'enseignement et de recherche français ou étrangers, des laboratoires publics ou privés.

Tailoring the Schiff Base Photoswitching – non-adiabatic molecular dynamics study of substituent effect on Excited State Proton Transfer[†]

Joanna Jankowska,^{*ab‡} Mario Barbatti,^c Joanna Sadlej,^b and Andrzej L. Sobolewski^a

Small molecular systems exhibiting Excited State Intramolecular Proton Transfer (ESIPT) attract considerable attention due to their possible role as ultrafast, efficient, and photostable molecular photoswitches. Here by means of static potential energy profiles scan and on-the-fly non-adiabatic dynamics simulations we study photodeactivation process of minimal-chromophore aromatic Schiff base, salicylidene methylamine (SMA), and its two derivatives 6-cyano-salicylidene methylamine (6-CN-SMA) and 3-hydroxy-salicylidene methylamine (3-OH-SMA). We show that the dominant character of the lowest excited singlet state – $\pi\pi^*$ vs. $n\pi^*$ – plays a crucial role for the system's photophysics and controls the ESIPT efficiency. We also show that the relative alignment of the $\pi\pi^*$ and $n\pi^*$ states may be controlled through chemical substitutions made to the aromatic ring of the Schiff-base molecule. We believe that our findings will improve the rational-design strategies employed for the ESIPT systems, especially in the context of their possible photoswitching.

1 Introduction

Excited state intramolecular proton transfer (ESIPT), an ultrafast photoinduced transformation in which a proton involved in an intramolecular hydrogen bonding moves between two electronegative centers, has recently given rise to an exciting, interdisciplinary field of study, attracting interest of chemists, physicists, and biologists¹. Acting at ultrashort timescales including even the femtosecond regime, ESIPT allows for a rapid redistribution of excitation energy and, thus, enhances the photostability of the excited molecular systems, giving rise to rich applications in the organic UV photostabilizers industry^{2–4}. ESIPT plays also a crucial role in the activity of photoacids and photobases^{5–7}; it occurs in photo-sensitive proteins^{8–11} and metal complexes;¹² and it is even considered among primary factors enabling the evolution of life, due to its role in nucleic-bases photochemistry^{13–15}. The photoinduced proton transfer, usually accompanied by a pronounced redistribution of the electronic density, results in large emission Stokes shifts, opening possibilities for bioluminescence

color tuning and, by creation of photochromism between potential meta-stable ground state isomers^{16–19}, enables selective molecular photoswitching and information storage²⁰.

Molecular switches, among other single molecule electronic units, are characterized as bi-stable systems in which reversible switching of various physical and chemical properties is achieved through exposure to external stimulus. The two forms of the switching molecule may differ by numerous attributes such as *cis-trans* isomerism^{21–24}, chirality²⁵, open-closed ring structure,^{26–28} or tautomeric structure^{29–33}. Up to date, the palette of experimentally studied factors allowing for the switching control includes an external electromagnetic irradiation^{21,26,34}, electric current transmission^{29,35}, static electric²² and magnetic²⁶ fields, short-range forces³⁶, temperature^{26,37}, chemical reactions,^{38,39} and mechanical stretching⁴⁰. Among other switching-triggering stimuli, light, allowing for ultrafast, remote and precise switching control, appears as especially promising and widely investigated trigger.

Among organic systems considered as potentially good candidates for molecular photoswitches, a family of α -hydroxy aromatic Schiff bases constitutes an important class of compounds, whose photophysical behavior can be attributed to the ESIPT process. From gas-phase experiments, it is known that the most stable ground state form of numerous model α -hydroxy Schiff bases corresponds to a *cis-enol* isomer^{41–43}, while the photochromic form is most likely an open-rotamer (*trans*) of keto character. The reaction coordinates linking the *cis-enol* and *trans-keto* forms may

^a Institute of Physics, Polish Academy of Sciences, 02-668 Warsaw, Poland

^b Faculty of Chemistry, University of Warsaw, 02-093 Warsaw, Poland

^c Aix Marseille Univ, CNRS, ICR, Marseille, France

^{*} Corresponding author; E-mail: jjank@ifpan.edu.pl

[†] Electronic Supplementary Information (ESI) available: ... See DOI: 10.1039/b000000x/

[‡] Present address: Department of Chemistry, University of Southern California, Los Angeles, CA 90089, USA

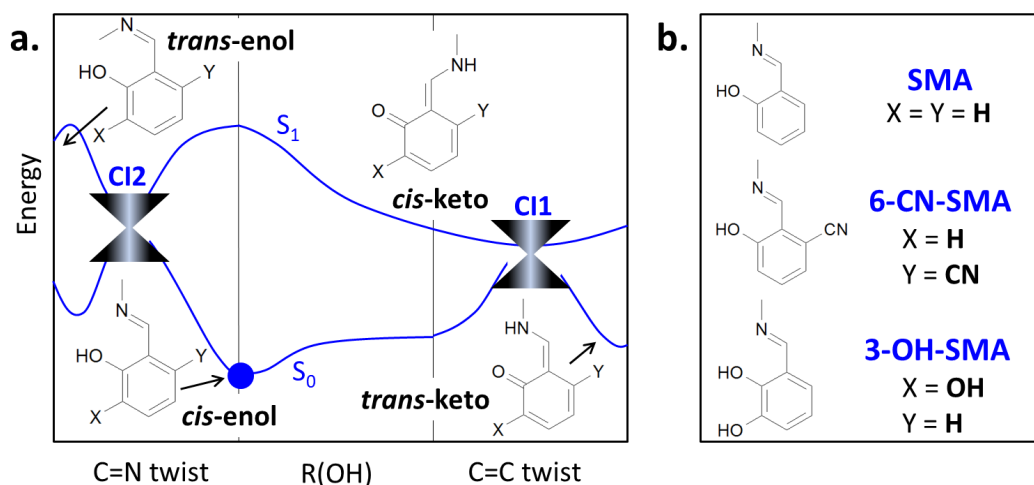


Fig. 1 General potential energy landscape along reaction coordinates crucial for the Schiff bases' photochemistry (a.) and global minimum structures of the three investigated compounds (b.). Blue dot shows the location of the global S_0 minimum (*cis-enol* form). 'C=N twist' and 'C=C twist' labels denote the dihedral rotation around the corresponding double bonds, the 'R(OH)' stands for the O-H distance in the hydrogen bonding and parametrizes the proton transfer reaction coordinate.

be identified as a proton transfer (PT) followed by a twist around the C=C bond (Fig. 1, part a.). As it has been shown elsewhere⁴⁴, these two coordinates built up a path for reversible molecular switching of a model, minimal photochromic Schiff base system – salicylidene methylamine (SMA). Moreover, the photochromism observed between the *cis-enol* and *trans-keto* isomers allows for their selective excitation, which is one of the key features enabling the optical control of a molecular photoswitch.

The present work consists of a combined static and dynamic computational study on the deactivation mechanism of the optically excited SMA molecule and its two derivatives: 6-CN-SMA and 3-OH-SMA. The proposed molecular systems have been designed to study the chemical substitution effect of the π -electron donor (-CN) and π -electron acceptor (-OH) groups on the time scale and efficiency of the α -hydroxy Schiff bases photodeactivation process (see Fig. 1, part b. for key geometrical structures). The analysis includes potential energy (PE) profiles scan along crucial reaction coordinates, followed by the on-the-fly non-adiabatic simulation; both performed at the TDDFT level of theory.

We show that, upon excitation to the lowest excited singlet state, S_1 , there are two main competing photodeactivation routes: through the excited state proton transfer followed by the out-of-plane structural transformation, and through the direct rotation around C=N bond. The former mechanism is found to play the leading role and its rate and efficiency show positive correlation with a $\pi\pi^*$ dominant character of the S_1 state. On the contrary, the alternative photodeactivation route is supported by stabilization of the $n\pi^*$ S_1 character. It is found that by means of structural modification one may control: (1) the ESIPT vs. C=N twist splitting ratio, (2) the accessibility of different conical intersections, and (3) barrierless vs. barrier-controlled ESIPT process. The obtained results not only broaden the understanding of the Schiff bases complex photochemistry, but also point out specific tools for tailoring their photophysical properties, rising new opportuni-

ties in the design of Schiff base molecular photoswitches.

2 Computational Methods

For each of the three investigated systems, a set of static PE profiles and on-the-fly non-adiabatic dynamics calculations were performed. In all cases, the electronic structure method chosen for the ground state exploration was density functional theory (DFT) with use of the Becke 3-parameter-Lee-Yang-Parr (B3LYP) hybrid functional^{45–47}, combined with the Dunning correlation-consistent double-zeta basis set with polarization and diffuse functions on all atoms (aug-cc-pVDZ)⁴⁸. The excited state energies and structures were obtained with the linear-response time-dependent density functional theory within the Tamm-Dancoff approximation (TD-DFT/TDA)⁴⁹ with the same functional and basis set. This computational method has been chosen for its quality performance^{50,51}, computational efficiency, and satisfactory stability in the vicinity of the encountered S_1/S_0 intersections, after testing a series of computationally affordable methods, including the full linear response TDDFT (with B3LYP, cam-B3LYP, and ω B97xD functionals) and the *ab initio* approaches CC2 and ADC(2). Results for the UV absorption spectra for the *cis-enol* form of the all studied systems are presented in Table 1.

The S_1/S_0 conical intersection points were also optimized at the complete active space self-consistent field approach averaged over two lowest singlet states and with six electrons in six orbitals (CASSCF(6,6)), with the cc-pVDZ basis set (for the optimized CI structures' coordinates see Tables S1–S3 in the ESI[†]).

Excited state dynamics, including non-adiabatic events up to the S_4 state, was performed with the fewest switches surface hopping approach (FSSH)⁵² including decoherence corrections⁵³. Non-adiabatic couplings between excited states were computed with the finite difference method proposed by Hammes-Schiffer and Tully⁵⁴ and implemented for TDDFT as explained in ref.⁵⁵, using the Casida ansatz⁵⁶ to represent the wavefunctions. Due to the limitations of DFT to describe the multireference character

Table 1 UV-Vis excitation energies of the *cis*-enol form calculated with aug-cc-pVDZ basis set on the B3LYP/aug-cc-pVDZ optimized geometry for SMA, 6-CN-SMA, and 3-OH-SMA. All DFT calculations were performed within the TD-DFT approach with the only exception of the reference TD-DFT/TDA/B3LYP/aug-cc-pVDZ data marked as TDA/B3LYP. For the B3LYP, CC2 and ADC(2) calculations the TURBOMOLE and for cam-B3LYP and ω B97xD the Gaussian09 suite of programs were employed. All values are expressed in eV. State character identification has been made on the basis of the orbital visualization. Reported oscillator strength values (f) have been obtained at the TD-DFT/TDA/B3LYP/aug-cc-pVDZ level of theory.

SMA	state	f	TDA/B3LYP	B3LYP	cam-B3LYP	ω B97xD	CC2	ADC(2)
	$S_1(\pi\pi^*)$	0.0172	4.13	4.00	4.31	4.32	4.17	4.13
	$S_2(n\pi^*)$	0.0067	4.70	4.67	4.95	4.94	4.98	4.89
	$S_3(\pi\pi^*)$	0.0484	5.10	4.92	5.16	5.18	5.23	5.18
6-CN-SMA	state	f	TDA/B3LYP	B3LYP	cam-B3LYP	ω B97xD	CC2	ADC(2)
	$S_1(\pi\pi^*)$	0.0082	4.00	3.86	4.15	4.15	4.02	3.99
	$S_2(n\pi^*)$	0.0050	4.42	4.39	4.75	4.73	4.74	4.65
	$S_3(\pi\pi^*)$	0.0268	4.91	4.72	4.96	4.98	5.16	5.10
3-OH-SMA	state	f	TDA/B3LYP	B3LYP	cam-B3LYP	ω B97xD	CC2	ADC(2)
	$S_1(\pi\pi^*)$	0.0269	3.80	3.68	4.10	4.11	3.95	3.91
	$S_2(\pi\pi^*)$	0.0445	4.79	4.66	4.94	4.97	5.05	4.96
	$S_3(n\pi^*)$	0.0075	4.88	4.76	5.01	5.00	5.06	5.02

of the ground state near the S_1/S_0 intersection, no couplings to the ground state were computed and the dynamics was stopped as soon as a S_1/S_0 energy gap equal or smaller than 0.15 eV was reached. This energy threshold was taken as an indicator of the internal conversion to the ground state as well. The advantages, as well as the limitations of surface hopping based on DFT to treat ultrafast non-adiabatic dynamics have been recently reviewed in ref.⁵⁷.

Each set of semi-classical dynamics simulations included 50 independent surface-hopping trajectories covering the first 500 fs of the photoinduced reaction with 0.5 fs time step set for the nuclear motion for which the velocity Verlet algorithm was applied to solve Newton's equations. The electronic equations were solved with 0.025 fs time-step, using interpolated energies and wavefunctions between two nuclear steps. The initial conditions for each trajectory were generated by sampling the coordinates and momenta so as to reproduce the ground-vibrational quantum harmonic distribution of the electronic ground state by means of a Wigner distribution⁵⁸. All trajectories started in the S_1 state. Reported transformation timescales were determined for 50% drop of the initial population within the chosen reaction channel. The transformation efficiencies correspond to percentage of trajectories that demonstrated occurrence of the transformation of interest at the moment of their termination; errors were estimated for 90% confidence interval.

The static calculations, including the ground and excited state minima optimizations together with the PE profiles and UV-Vis absorption spectra calculations were performed with the TURBOMOLE (version 6.3)⁵⁹ program package (with B3LYP) and with Gaussian 09⁶⁰ (with cam-B3LYP and ω B97xD). CASSCF calculations were done with the Gaussian 09 program, too. Surface hopping dynamics simulations were done with Newton-X (version 1.4.1)^{61,62} interfaced with TURBOMOLE.

3 Results and Discussion

Preliminary check of the potential energy profiles

As the first step of the photodeactivation study, we calculated static PE profiles along the crucial reaction coordinates for the three selected Schiff base systems (see Fig. 2). For the bare SMA molecule (Fig. 2, part a.) and the 6-CN-SMA derivative (b.), the calculations covered PT path from *cis*-enol to *cis*-keto form controlled by the OH-distance coordinate (R(OH)); the subsequent rotation around the C=C bond (C=C twist, from *cis*-keto to *trans*-keto); and the alternative route involving the C=N bond rotation (C=N twist, from *cis*-enol to *trans*-enol). In the case of the 3-OH-SMA derivative (parts c. and d.), the PE profiles additionally included the second PT transfer between the oxygen atoms, parametrized by the R(OH)(2) coordinate controlling the distance of the hydrogen atom and the proton-donating oxygen, and subsequent multidimensional relaxation parameterized by the rotation around the C=C bond. All profiles were determined at geometries optimized for the lowest excited singlet state (S_1) within the C_1 symmetry, except for the PT reaction paths which were calculated within C_s symmetry in order to eliminate unphysical coupling of the ultrafast PT transformation with the much slower out-of-plane molecular deformations (such as C=C rotation).

Upon examination of parts a.-c. in Fig. 2, one finds that vertical excitation of the global ground state minimum (*cis*-enol form) brings the Schiff system to the S_1 state in which, subsequently, two competing transformations may occur: ESIPT (middle panel of a.-c.) or direct rotation around C=N bond in the methylimine group (left panel of a.-c.). Both processes are found exoergic, with a similar energy gain of ca. 0.6 eV. The former leads towards an excited state local minimum (*cis*-keto form), while the latter drives the system to a S_1/S_0 intersection, denoted as CI2

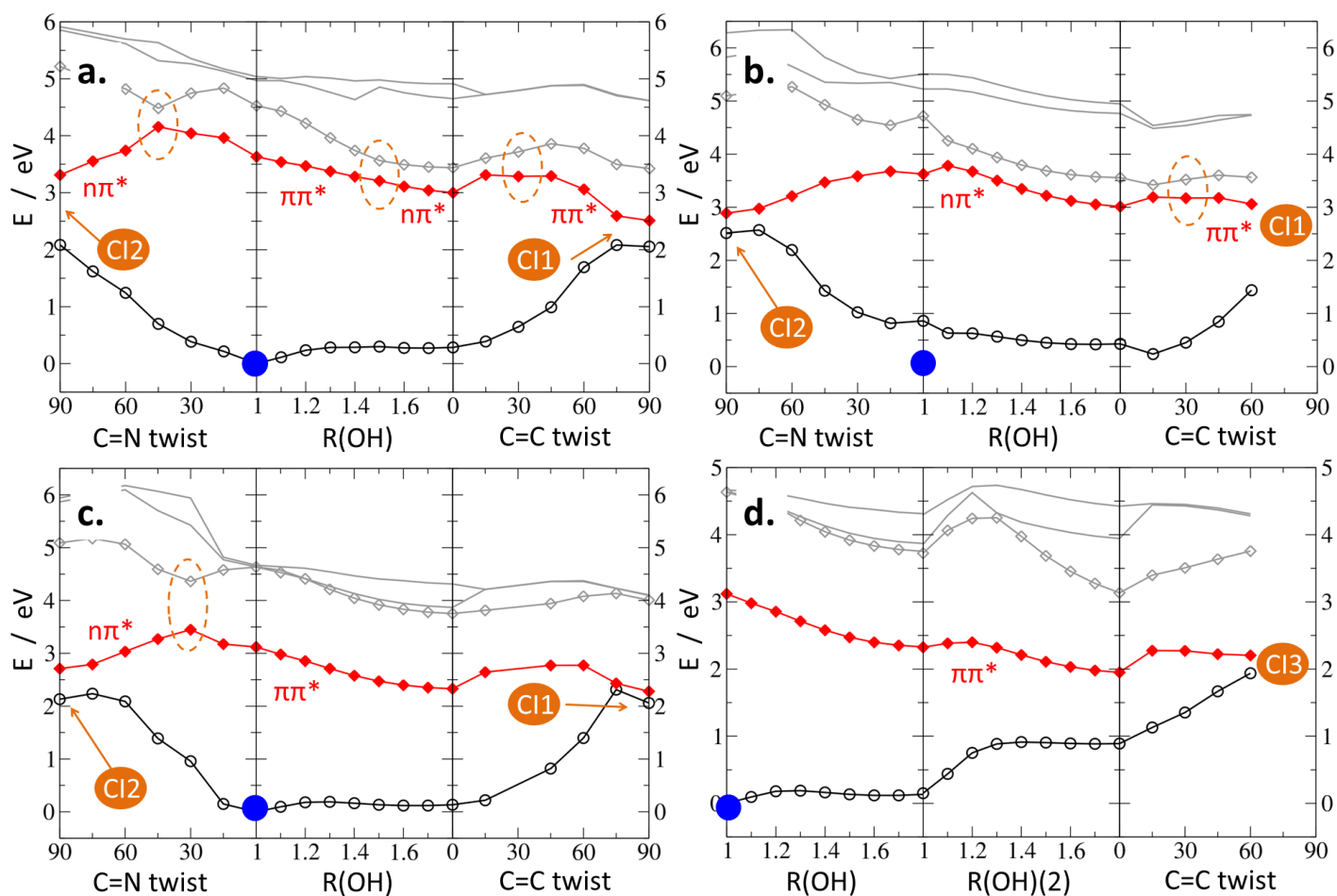


Fig. 2 PE profiles along photophysically relevant reaction coordinates for SMA (a.), 6-CN-SMA (b.), and 3-OH-SMA (c., d.) systems. All energies have been calculated on S_1 -optimized structures. Color coding: S_0 state - empty black circles, S_1 - full red diamonds, S_2 - empty gray diamonds, S_3 , S_4 - solid gray lines. Current dominant character of the S_1 state has been marked as red labels. Orange dotted circles mark S_1 character change regions. Full orange circles indicate intersections (CIs) of particular type. Blue dot shows the location of the global S_0 minimum (*cis*-enol form).

and corresponding to the perpendicular orientation of the methyl group with respect to the aromatic ring (see Fig. S3 in the ESI[†] for CI2 points' structures). The preference for the particular photoreaction route is expected to originate primarily from the energy barriers encountered in the Franck-Condon (FC) region in the S_1 state. These barriers depend on the dominant character of the S_1 state and, therefore, on the chosen chemical substituents. The distinction between the $\pi\pi^*$ and $n\pi^*$ state characters within the C_1 symmetry regions is made on the basis of the $S_0 \rightarrow S_x$ optical transition oscillator strength and through check of the electric dipole moment continuity along the reaction path. Both sets of data for all studied systems are presented Figs. S1-S2 in ESI[†].

For the bare SMA molecule and for the π -electron donating OH substitution (3-OH-SMA), the $\pi\pi^*$ character of the S_1 state is dominant. This results in a barrierless profile along the ESIPT transformation for the both systems. On the contrary, the alternative C=N rotation path shows an energy barrier of ca. 0.5 eV in the $\pi\pi^*$ state. It has been also observed that dominant $n\pi^*$ character of the S_1 state is necessary to reach the CI2 intersection point (see Fig. 2), thus a state switch character is needed in the SMA and 3-OH-SMA systems in order to follow this reaction path. The situation is reversed for the CN substitution withdrawing the π -electron density from the aromatic ring. In the case of the 6-CN-SMA molecule, the FC region around the ground-state PE global minimum in S_1 shows dominant $n\pi^*$ character. This comes along with rise of the energy barrier for the ESIPT process up to ca. 0.3 eV and with effectively barrierless access from the FC region to the CI2 point through the C=N bond rotation.

The ESIPT transformation, driving the Schiff molecule to its *cis*-keto form, opens various scenarios for subsequent photochemical reactions. Right panels of Fig. 2 a.-c. illustrate the PE profiles along C=C bond rotation coordinate connecting the *cis*-keto region with CI1 intersection, corresponding to the perpendicular orientation if the N-CH₃ moiety with respect to the aromatic ring (for the CI point's structure see Fig. S3 in the ESI[†]). It turns out that this transformation requires dominant $\pi\pi^*$ character of the S_1 state and, depending on the substitution, needs up to 0.3 eV to overcome the potential energy barrier. The beneficial influence of the $\pi\pi^*$ excitation might be associated with weakening of the C=C bond due to depopulation of the bonding π orbital and concordant population of the antibonding π^* star orbital localized on the same bond.

In the case of the 3-OH-SMA system, the ESIPT process can be also followed by the second PT, occurring between the oxygen atoms, as shown in Fig. 2 d. (middle panel). This transformation involves passing over a small energy barrier (less than 0.15 eV) and results in pronounced reduction of the S_1/S_0 energy gap. The second ESIPT may be further followed by multidimensional out-of-plane structural relaxation, parameterized in the right panel of Fig. 2 d. by C=C rotation, leading to another S_1/S_0 intersection, CI3, characterized by moderate out-of-plane distortion of the N-CH₃ group accompanied with some pyramidalization of the N atom (for the CI point's structure see Fig. S3 in the ESI[†]).

The static results discussed in this part of the study stay in good agreement with ADC(2)/cc-pVDZ fully relaxed PE surface exploration reported in ref. ⁶³.

Results of photodynamical simulations

The static photodeactivation study of SMA, 6-CN-SMA, and 3-OH-SMA systems constitutes ground for the non-adiabatic surface hopping investigation of their photodynamics. The aim of the dynamic simulations is, on the one hand, to verify the expected directions of photo-induced reactions, supplementing the static analysis with the nuclear kinetic effects and, on the other hand, to estimate the characteristic timescales of particular photo-transformations.

Fig. 3 presents the time evolution of the population for the three studied Schiff systems (parts a.-c.) and Fig. 4 gathers characteristic timescales and reaction efficiencies extracted from the simulations. In all cases the dynamic study reveals low contributions from higher excited states, showing the dominant role of the S_1 state in the ongoing photo-transformations. It may be observed that the ESIPT significantly dominates over alternative C=N rotation route. The exact splitting ratio between these two reactions depends on the system: the CN-substitution supports the C=N rotation mechanism, while presence of the OH-substituent closes this reaction path entirely (see Fig. 4 for numerical results). In terms of rates, the proton transfer process, defined as structural transformation in which mean proton distance to proton-donor moiety becomes larger than the mean proton distance to the proton-acceptor group, occurs ultrafast in all cases: PT is finalized within ca. 10 fs after the excitation in the SMA and 3-OH-SMA systems, and within 20 fs in 6-CN-SMA (see Fig. 3, part d.), which shows excellent agreement with the reported wave packet dynamics result (11 fs)⁶⁴ and MRCI/OM2 value (30 fs)⁶⁵ for PT in SMA. The C=N rotation, if occurs, drives the system efficiently to the CI2 conical intersection point within 160 fs and 140 fs for the SMA and 6-CN-SMA systems, respectively. The large rate difference between the PT and C=N twist observed for the both compounds underlines the role of momentum of inertia of the rotating group and low mass of the moving proton, which – together with energy barriers on PE surfaces – constitute important factors affecting the splitting ratio between the competing reaction routes.

Upon analysis of Fig. 3 b. a sudden drop of the S_1 population can be observed. The S_1 depopulation of 38% taking place at about 232 fs is balanced by a complementary raise of the S_2 population. This happens because a subset of 11 trajectories smoothly and simultaneously acquire a $\pi\pi^*$ character, with this state still in the S_2 position. This coherent motion seems to be correlated to the N atom pyramidalization, which mixes the $n\pi^*$ and $\pi\pi^*$ states. During the next 50 fs, all these trajectories hop back to S_1 .

In line with the static study predictions, after the ESIPT process various subsequent transformations are observed. In all systems, a significant number of trajectories leads, through the C=C twist, to the main intersection point, CI1. The efficiency and rate of this reaction depend on the substituent and are found to be strongly hindered by the CN group insertion (see Fig. 4; note that the reported reaction-step efficiencies are conditional and assume fulfillment of the necessary preceding steps, e.g. CI1 efficiency refers to the percentage of ESIPT trajectories, which reached the CI1 intersection). This is associated with the stabilization of the $n\pi^*$ character of the S_1 state in this system, unfavorable to the C=C

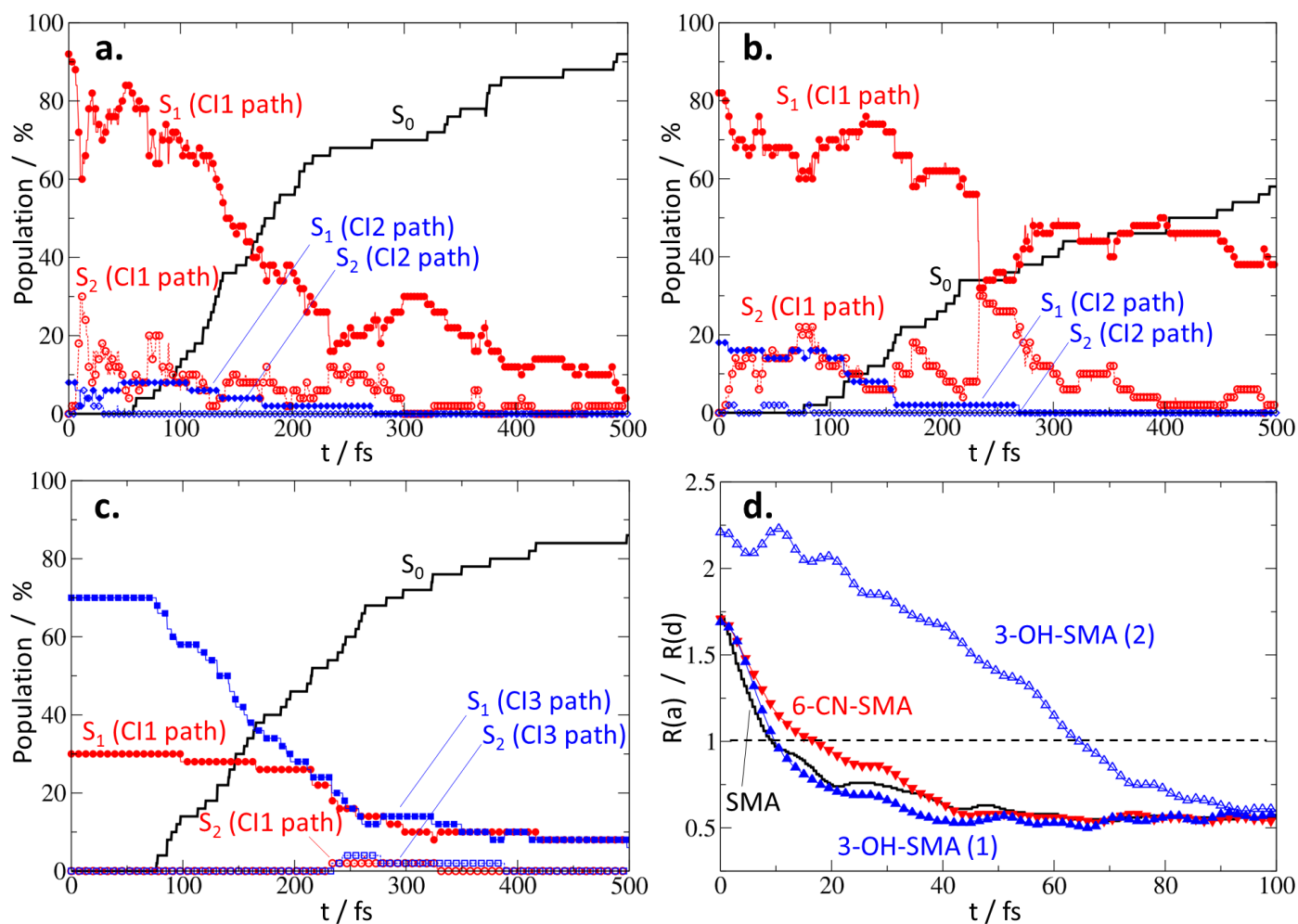


Fig. 3 FSSH electronic state populations (a., b., c.) and proton transfer (d.) dynamics in all studied systems: (a.) – SMA, (b.) – 6-CN-SMA, and (c.) – 3-OH-SMA. Color coding: (a., b.) black line - S_0 population, red full/empty circles - S_1/S_2 population along the CI1 path, blue full/empty diamonds - S_1/S_2 population along the CI2 path, (c.) black - S_0 population, red full/empty circles - S_1/S_2 population along the CI1 path, blue full/empty squares - S_1/S_2 population along the CI3 path, (d.) ratio of the mean proton-donor ($R(d)$) distance over the mean proton-acceptor ($R(a)$) distance along the dynamics for all studied systems: black - SMA, red full down-triangles - 6-CN-SMA, blue full/empty up-triangles - first/second PT in 3-OH-SMA.

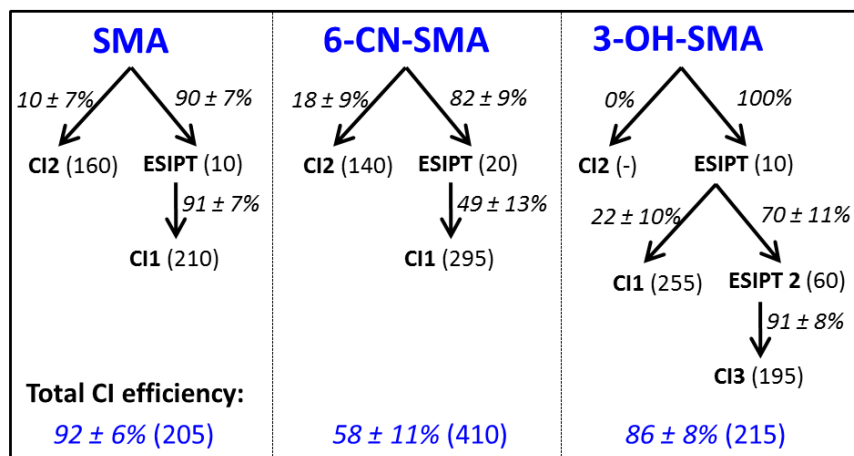


Fig. 4 Non-adiabatic dynamics results for deactivation paths efficiencies (italic) and time decay constants (in brackets, expressed in fs).; the reported errors were estimated for 90% confidence interval.

rotation. Again, the results obtained for the bare SMA system stay in a very good agreement with the MRCI/OM2 results from the semi-empirical study of the full SMA-molecule photoswitching process⁶⁵.

The second PT transformation, ESIPT 2, happening on average ca. 50 fs after the first PT, plays an important role in the 3-OH-SMA molecule photodeactivation scheme, present in vast majority of the calculated dynamic trajectories. Subsequent out-of-plane relaxation driving the system to the CI3 point shows efficiency similar to the C=C rotation towards CI1 occurring after the first ESIPT, but is characterized by a faster decay timescale (195 vs. 255 fs), which originates most probably from the lower energy barrier for the out-of-plane transformation.

Gathering together the observed photoreaction routes and taking into account their timescales, it can be concluded that isolated aromatic Schiff base molecules, depending on chosen substituents, may undergo ultrafast and efficient deactivation. The best characteristics is found for the bare SMA system which achieves $92 \pm 6\%$ ground state population with 205 fs lifetime of the total excited states' population; similar result is found for the OH-substituted SMA, $86 \pm 8\%$ and 215 fs. On the contrary, in the CN-substituted system, attenuation of the leading ESIPT and C=C twist deactivation mechanism is observed, giving rise to much longer excited state lifetime of 410 fs, comparable to the overall time of the performed simulation.

It is worth mentioning that the discussed results make a consistent picture of the Schiff bases' photodynamics when compared to properties of another simple Schiff base molecule, salicylidene aniline (SA), reported recently by Spörkel et al.⁶⁶. First of all, one finds very good agreement between the calculated characteristic timescales, such as the PT rate (several tens of femtoseconds) or the mean system's photodeactivation time (150 – 250 fs). Secondly, only one photodeactivation route is observed for the SA system: the one involving ESIPT followed by the C=C twist transformation (CI1 path). It should be noticed that, in similarity to the 3-OH-SMA molecule, the SA system also shows stabilized $\pi\pi^*$ character of the S_1 state. Thus, the observed total closure of the competing C=N twist route stays in line with the mechanistic picture proposed herein.

4 Conclusions

In summary, we performed a joined static and dynamic computational study on the deactivation mechanism of the optically excited SMA system and its two derivatives, 6-CN-SMA and 3-OH-SMA. The analysis included PE profile scan along crucial reaction coordinates, followed by the on-the-fly non-adiabatic simulation; both performed at the TDDFT level of theory. The particular choice of the CN- and OH-derivatives of the model Schiff-base SMA molecule has been made on the basis of their opposite influence on the π -electron density. Our results provide insights into the nature of the ESIPT-based photochemistry of aromatic Schiff bases and characterize their leading photodeactivation mechanisms.

We show that, upon excitation to the lowest excited singlet state, there are two main competing photodeactivation routes: through the excited state proton transfer followed by the out-of-

plane structural transformation (such as twist around C=C bond), and through the direct rotation around C=N bond. The former plays a dominant role in all studied Schiff systems and its efficiency and rate increase along with the stabilization of the $\pi\pi^*$ character of the S_1 state. On the contrary, the alternative photodeactivation route is enhanced by stabilization of the $n\pi^*$ S_1 character. Tailoring of the lowest excited state character can be achieved through chemical substitutions applied to the aromatic ring of the Schiff base molecule: the π -electron donating OH group stabilizes the $\pi\pi^*$ lowest excitation character, while the π -electron accepting CN group endorses the $n\pi^*$. By means of such structural modification one may control the ESIPT vs. C=N twist transformation splitting ratio, accessibility of different intersections (CI1 – supported by $\pi\pi^*$ and CI2 – supported by $n\pi^*$), and barrierless or barrier-controlled ESIPT character, which – altogether – opens new and wide palette of opportunities in the design of Schiff base molecular photoswitches.

Acknowledgement

MB thanks the support of the A*MIDEX grant (n° ANR-11-IDEX-0001-02) and of the project Equip@Meso (ANR-10-EQPX-29-01), both funded by the French Government "Investissements d'Avenir" program. ALS acknowledges the support of the National Science Center of Poland, grant no. 2012/04/A/ST2/00100. JJ gratefully acknowledges the Max-Planck-Institut für Kohlenforschung (Mülheim an der Ruhr, Germany) for generous computer time allocation.

References

- 1 P.-T. Chou and K. M. Solntsev, *J. Phys. Chem. B*, 2015, **119**, 2089.
- 2 J. E. Otterstedt, *J. Chem. Phys.*, 1973, **58**, 5716.
- 3 H. J. Heller and H. R. Blattmann, *Pure Appl. Chem.*, 1972, **30**, 145.
- 4 L. A. Baker, M. D. Horbury, S. E. Greenough, M. N. R. Ashfold and V. G. Stavros, *Photochem. Photobiol. Sci.*, 2015, **14**, 1814.
- 5 C. Spies, S. Shomer, B. Finkler, D. Pines, E. Pines, G. Jung and D. Huppert, *Phys. Chem. Chem. Phys.*, 2014, **16**, 9104.
- 6 D. Pines, E. T. J. Nibbering and E. Pines, *Isr. J. Chem.*, 2015, **55**, 1240.
- 7 S. P. Laptенок, J. Conyard, P. C. B. Page, Y. Chan, M. You, S. R. Jaffrey and S. R. Meech, *Chem. Sci.*, 2016, **7**, 5747.
- 8 R. B. Vegh, D. A. Bloch, A. S. Bommarius, M. Verkhovskiy, S. Pletnev, H. Iwaï, A. V. Bochenkova and K. M. Solntsev, *Phys. Chem. Chem. Phys.*, 2015, **17**, 12472.
- 9 M. Kaucikas, M. Tros and J. J. Van Thor, *J. Phys. Chem. B*, 2015, **119**, 2350.
- 10 R. Chowdhury, A. Saha, A. K. Mandal, B. Jana, S. Ghosh and K. Bhattacharyya, *J. Phys. Chem. B*, 2014, **119**, 2149.
- 11 T. Chatterjee, F. Lacombat, D. Yadav, M. Mandal, P. Plaza, A. Espagne and P. K. Mandal, *J. Phys. Chem. B*, 2016, **120**, 9716.
- 12 O. S. Wenger, *Coord. Chem. Rev.*, 2015, **282-283**, 150.
- 13 C. Ko and S. Hammes-Schiffer, *J. Phys. Chem. Lett.*, 2013, **4**, 2540.

- 14 K. Röttger, H. J. B. Marroux, M. P. Grubb, P. M. Coulter, H. Böhnke, A. S. Henderson, M. C. Galan, F. Temps, A. J. Orr-Ewing and G. M. Roberts, *Angew. Chemie - Int. Ed.*, 2015, **54**, 14719.
- 15 Y. Zhang, K. De La Harpe, A. A. Beckstead, R. Improta and B. Kohler, *J. Am. Chem. Soc.*, 2015, **137**, 7059.
- 16 K. Kownacki, A. Mordziński, R. Wilbrandt and A. Grabowska, *Chem. Phys. Lett.*, 1994, **227**, 270.
- 17 Y. Eichen, J.-M. Lehn, M. Scherl, D. Haarer, J. Fischer, A. Decian, A. Corval and H. P. Trommsdorff, *Angew. Chem. Int. Edit.*, 1995, **34**, 2530.
- 18 S. Møller, K. B. Andersen, J. Spanget-Larsen and J. Waluk, *Chem. Phys. Lett.*, 1998, **291**, 51.
- 19 G. Wiosna-Sałyga, J. Dobkowski, M. M. S., I. Sazanovich, R. P. Thummel and J. Waluk, *Chem. Phys. Lett.*, 2006, **423**, 288.
- 20 S. Silvi, A. Arduini, A. Pochini, A. Secchi, M. Tomasulo, F. M. Raymo, M. Baroncini and A. Credi, *J. Am. Chem. Soc.*, 2007, **129**, 13378.
- 21 K. G. Yager and C. J. Barrett, *J. Photoch. Photobio. A*, 2006, **182**, 250.
- 22 M. Alemani, M. V. Peters, S. Hecht, K.-H. Rieder, F. Moresco and L. Grill, *J. Am. Chem. Soc.*, 2006, **128**, 14446.
- 23 E. Ludwig, T. Strunskus, S. Hellmann, A. Nefedov, C. Wöll, L. Kipp and K. Rossnagel, *Phys. Chem. Chem. Phys.*, 2013, **15**, 20272.
- 24 D. Taherinia and C. D. Frisbie, *J. Phys. Chem. C*, 2016, **120**, 6442.
- 25 B. L. Feringa, R. A. van Delden, N. Koumura and E. M. Geertsema, *Chem. Rev.*, 2000, **100**, 1789.
- 26 M. Irie, *Chem. Rev.*, 2000, **100**, 1685.
- 27 J. Massaad, Y. Coppel, M. Sliwa, M. L. Kahn, C. Coudret and F. Gauffre, *Phys. Chem. Chem. Phys.*, 2014, **16**, 22775.
- 28 S. L. Broman and M. B. Nielsen, *Phys. Chem. Chem. Phys.*, 2014, **16**, 21172.
- 29 P. Liljeroth, J. Repp and G. Meyer, *Science*, 2007, **317**, 1203.
- 30 J. Waluk and E. Vogel, *J. Phys. Chem.*, 1994, **98**, 4530.
- 31 A. L. Sobolewski and W. Domcke, *Phys. Chem. Chem. Phys.*, 2006, **8**, 3410.
- 32 A. L. Sobolewski, *Phys. Chem. Chem. Phys.*, 2008, **10**, 1243.
- 33 L. Łapiński, M. J. Nowak, J. Nowacki, M. F. Rode and A. L. Sobolewski, *ChemPhysChem*, 2009, **10**, 2290.
- 34 G. Berkovic, V. Krongauz and V. Weiss, *Chem. Rev.*, 2000, **100**, 1741.
- 35 V. Iancu and S.-W. Hla, *P. Natl Acad. Sci. USA*, 2006, **103**, 13718.
- 36 C. Loppacher, M. Guggisberg, O. Pfeiffer, E. Meyer, M. Bamberlin, R. Lüthi, R. Schlittler, J. K. Gimzewski, H. Tang and C. Joachim, *Phys. Rev. Lett.*, 2003, **90**, 066107.
- 37 M. Piantek, G. Schulze, M. Koch, K. J. Franke, F. Leyssner, A. Krüger, C. Navío, J. Miguel, M. Bernien, M. Wolf, W. Kuch, P. Tegeder and J. I. Pascual, *J. Am. Chem. Soc.*, 2009, **131**, 12729.
- 38 J. Wook Lee, K. Kim and K. Kim, *Chem. Commun.*, 2001, 1042.
- 39 Z. L. Pianowski, J. Karcher and K. Schneider, *Chem. Commun.*, 2016, **52**, 3143.
- 40 S. V. Aradhya and L. Venkataraman, *Nat. Nano*, 2013, **8**, 399.
- 41 M. Ziółek, J. Kubicki, A. Maciejewski, R. Naskręcki and A. Grabowska, *Chem. Phys. Lett.*, 2003, **369**, 80.
- 42 A. Grabowska, K. Kownacki and L. Kaczmarek, *Acta Phys. Pol. A*, 1995, **88**, 1081.
- 43 M. I. Knyazhansky, A. V. Metelitsa, M. E. Kletskii, A. A. Millov and S. O. Besugliy, *J. Mol. Struct.*, 2000, **526**, 65.
- 44 J. Jankowska, M. F. Rode, J. Sadlej and A. L. Sobolewski, *ChemPhysChem*, 2012, **13**, 4287.
- 45 C. Lee, W. Yang and R. G. Parr, *Phys. Rev. B*, 1988, **37**, 785.
- 46 A. D. Becke, *J. Chem. Phys.*, 1993, **98**, 5648.
- 47 P. J. Stephens, F. J. Devlin, C. F. Chabalowski and M. J. Frisch, *J. Phys. Chem.*, 1994, **98**, 11623.
- 48 R. A. Kendall, T. H. Dunning and R. J. Harrison, *J. Chem. Phys.*, 1992, **96**, 6796.
- 49 S. Hirata and M. Head-Gordon, *Chem. Phys. Lett.*, 1999, **314**, 291.
- 50 A. L. Sobolewski and W. Domcke, *Phys. Chem. Chem. Phys.*, 1999, **1**, 3065.
- 51 Y. Houari, S. Chibani, D. Jacquemin and A. D. Laurent, *J. Phys. Chem. B*, 2015, **119**, 2180.
- 52 J. C. Tully, *J. Chem. Phys.*, 1990, **93**, 1061.
- 53 G. Granucci and M. Persico, *J. Chem. Phys.*, 2007, **126**, 134114.
- 54 S. Hammes-Schiffer and J. C. Tully, *J. Chem. Phys.*, 1994, **101**, 4657.
- 55 M. Barbatti, J. Pittner, M. Pederzoli, U. Werner, R. Mitrić, V. Bonačić-Koutecký and H. Lischka, *Chem. Phys.*, 2010, **375**, 26.
- 56 M. E. Casida, *Recent advances in density functional methods, Part I*, World Scientific, Singapore, 1995, p. 155.
- 57 M. Barbatti and R. Crespo-Otero, *Top. Curr. Chem.*, 2015, **368**, 415.
- 58 M. Barbatti and K. Sen, *Int. J. Quantum Chem.*, 2016, **116**, 762.
- 59 *TURBOMOLE V 6.3 2011, a development of University of Karlsruhe and Forschungszentrum Karlsruhe GmbH, 1989-2007, TURBOMOLE GmbH, since 2007; available from <http://www.turbomole.com>.*
- 60 M. J. et al. Frisch, *Gaussian 09 Revision C.01*, Gaussian Inc. Wallingford CT 2009.
- 61 M. Barbatti, M. Ruckebauer, F. Plasser, J. Pittner, G. Granucci, M. Persico and H. Lischka, *Wiley Interdiscip. Rev. Comput. Mol. Sci.*, 2014, **4**, 26.
- 62 M. Barbatti, G. Granucci, M. Ruckebauer, F. Plasser, J. Pittner, M. Persico and H. Lischka, *Newton-X: a package for Newtonian dynamics close to the crossing seam, version 1.4*, www.newtonx.org, 2013.
- 63 J. Jankowska, M. F. Rode, J. Sadlej and A. L. Sobolewski, *ChemPhysChem*, 2014, **15**, 1643.
- 64 J. M. Ortiz-Sánchez, R. Gelabert, M. Moreno and J. M. Lluch, *J. Phys. Chem. A*, 2006, **110**, 4649.

- 65 L. Spörkel, J. Jankowska and W. Thiel, *J. Phys.Chem. B*, 2015, **119**, 2702.
- 66 L. Spörkel, G. Cui and W. Thiel, *J. Phys. Chem. A*, 2013, **117**, 4574.